Quantum vibrational analysis of hydrated ions using an *ab initio* potential.

Eugene Kamarchik[a,b] and Joel M. Bowman[b]

[a] Department of Chemistry, University of Southern California,
Los Angeles, CA 90089-0482, USA

[b] C.L. Emerson Center for Scientific Computation, Dept. of Chemistry,
Emory University, Atlanta, GA 30322

(Dated: August 29, 2010)

We present full-dimensional potential energy surfaces (PESs) for hydrated chloride based on the sum of *ab initio* $(H_2O)Cl^-$, $(H_2O)_2$, and $(H_2O)_3$ potentials. The PESs are shown to predict minima and corresponding harmonic frequencies accurately based on comparisons with previous and new *ab initio* calculations for $(H_2O)_2Cl^-$, $(H_2O)_3Cl^-$, and $(H_2O)_4Cl^-$. An estimate of the effect of the 3-body water interaction is made using a simple 3-body water potential that was recently fit to tens of thousands of *ab initio* 3-body energies. Anharmonic, coupled vibrational calculations are presented for these two clusters, using the "local monomer model" for the high frequency intramolecular modes. This model is tested against previous "exact" calculations for $(H_2O)Cl^-$. Radial distribution functions at 0 K obtained from quantum zero-point wavefunctions are also presented for the $(H_2O)_2Cl^-$ and $(H_2O)_3Cl^-$ clusters.

I. INTRODUCTION

Electrolyte solutions play a central role in many chemical and biological processes including acid-base equilibria and ion transport. [1, 2] The understanding of the solvation process and its effects on the structure of water have consequently been the subject of intense experimental and theoretical interest for over 100 years. [3, 4] Despite this interest, electrolyte solutions remain challenging systems for which numerous questions have not been adequately answered. For instance, recent studies have focused on the controversy relating to the presence or absence of alkali and halide ions at the air-water interface. [5–10]

A variety of potentials that attempt to describe the solvation of ions have been developed for use in statistical mechanics or molecular dynamics simulations. Most of these potentials use rigid water monomers and simple descriptions of the interaction with the cation or anion under consideration, e.g., two-body interactions based on partial charges and damped Coulomb interactions. The more sophisticated versions of such models have been extended to include long-range many-body polarization[5, 11–16]. However, even these models may still fail to capture all of the effects associated with short-range 3-body terms and many limit the fundamental "flexibility" of the water monomer. As one alternative, "direct dynamics" approaches have become quite popular. In these approaches the potential energy for a specified configuration in a classical molecular dynamics simulation is computed using electronic structure methods[17–20]. Unfortunately, the necessity of performing repeated electronic structure calculations limits both the level of treatment and the length of the simulation, and so these method may not correctly describe important intramolecular forces such as dispersion.

Infrared spectroscopy is a particularly useful tool for studying water and electrolyte solutions, since it contains information about both structure and dynamics. In particular, the strong band due to the hydrogen-bonded OH stretch occuring at and below about 3500 cm^{-1} provides a signature of the hydrogen-bonding environments experienced by the water monomer. Interactions with neighboring waters as well as charged ions lead to experimentally measurable shifts in the line peak, which have been measured for solutions of NaCl, NaBr, and NI, among others. [21–23] The rigorous simulation of these spectra is of course a daunting task, starting with the potential and proceeding with rigorous, i.e., quantum, vibrational calculations. (See the interesting recent work by Skinner an co-workers on applying a local-mode model for this purpose. [24–27])

In this paper, we address both aspects of this task and as a first relevant case consider hydration of the ubiquitous chloride ion. First, we develop new chloride-water potentials based on a many-body approach. Direct computation of an *ab initio* potential for an electrolyte solution is a difficult task that is far beyond present computational capabilities. However, the calculation of 1-, 2-, and even 3-body potentials for various interacting species has become fairly routine within our approach[28]. Previously, we have developed *ab initio* full-dimensional potentials which accurately describe the 1-, 2-, and 3-body interactions of water monomers. [29–32] In addition, we have previously developed an *ab initio*, full-

dimensional potential that describes the interaction of a chloride ion with a single water monomer[33]. Here we present two new potentials: one relying only on 2-body potentials and a second which uses a 2-body term to describe the chloride-water interaction and an additional 3-body term to describe the water-water interaction. Second, to address the vibrational dynamics we apply the local-monomer model that we have developed for the calculation of vibrational energies of intramolecular modes. [34] A very similar model has also been developed by Halonen and co-workers for the water dimer, water trimer, and the H_2O-NO complex,[35–37] but our implementation is somewhat different than theirs. We also show how our model may be used to calculate radial distribution functions.

The paper is organized as follows. In the next section we present the new potential derived from the combination of our previous PESs. In the subsequent section we compare harmonic results and stationary geometries using these surfaces with results obtained by electronic structure methods. We also employ the local-monomer model in a post-harmonic analysis of the vibrational energies and the computation of radial distribution functions (RDFs). Finally, we present some conclusions and offer some posibilities for future work.

II. POTENTIAL FOR HYDRATED CHLORIDE

The PES for a hydrated chloride anion (and in general for any ion) with N water monomers can be represented as a many-body potential in the following way:

$$\begin{aligned} V(0_{\mathrm{Cl}}, 1_{\mathrm{H_2O}}, 2_{\mathrm{H_2O}}, \ldots, N_{\mathrm{H_2O}}) \;=\; & V(0_{\mathrm{Cl}}) + \sum_{i=1}^{N} V_{1-\mathrm{body}}(i_{\mathrm{H_2O}}) \\ & + \sum_{i=1}^{N} V(0_{\mathrm{Cl}}, i_{\mathrm{H_2O}}) + \sum_{i=1}^{N}\sum_{j>i}^{N} V_{2-\mathrm{body}}(i_{\mathrm{H_2O}}, j_{\mathrm{H_2O}}) \\ & + \sum_{i=1}^{N}\sum_{j>i}^{N}\sum_{k>j}^{N} V_{3-\mathrm{body}}(i_{\mathrm{H_2O}}, j_{\mathrm{H_2O}}, k_{\mathrm{H_2O}}) \\ & + \text{higher order terms.} \end{aligned} \tag{1}$$

Here 0 denotes the Cartesian coordinates of the chloride anion and 1 through N denote the collective Cartesian coordinates of the first through the Nth water monomer. We have employed two different versions of this potential, one in which we truncate at 2-body terms and a second in which 3-body water terms are included. The 1-body terms $V(O_{\mathrm{Cl}})$ and $V_{1-\mathrm{body}}(i_{\mathrm{H_2O}})$ and the chloride-water interaction term $V(0_{\mathrm{Cl}}, i_{\mathrm{H_2O}})$ are taken from the pre-

viously published water-chloride potential, based on fitting thousands of coupled cluster (CCSD(T)) energies. [33] The 2-body term describing the pairwise interaction of water monomers, $V_{2-\mathrm{body}}(i_{\mathrm{H_2O}}, j_{\mathrm{H_2O}})$ is taken from our high-accuracy water potential, again based on fitting thousands of CCSD(T) energies. [29] Finally, for the water 3-body term we adopt the functional form given by Kumar and Skinner [38] which was fit to our database of trimer electronic energies. [34]

Vibrational spectroscopy represents an important tool which can be used to experimentally distinguish between differently hydrated structures. A variety of methods for calculating vibrational energies exist, from full-mode, fully-coupled vibrational configuration-interaction (VCI) [39] to simple harmonic approximations. [40] Because we wish to focus on larger clusters we have eschewed the computationally demanding full-mode VCI in favor of an approximate method which accounts for the local environment around each water monomer. We term this model the "local-monomer model". [34] The local-monomer model (LMM) solves the Schrödinger equation for the vibrational motion of one monomer in the potential defined by the rest of the system. Within this model, the Schrödinger equation for each monomer is given by

$$[T_m + U_m(\mathbf{Q}_m) - \epsilon_{n_m}]\chi_m(\mathbf{Q}_m) = 0, \tag{2}$$

where $\mathbf{Q}_m$ denotes the intramolecular normal-modes modes associated with monomer m, T_m is the "exact" kinetic energy operator, and U_m is the potential of the monomer in the field defined by the rest of the system which is held fixed. For these calculations we choose $\mathbf{Q}_m$ to be the intramolecular modes in Cartesian coordinates obtained from a normal-mode analysis of the monomer of interest, with the remaining system held fixed. For the kinetic energy operator, T_m, we employ the kinetic energy from the Watson Hamiltonian, including the vibrational angular momentum terms. [41] The total vibrational energy and wavefunction of the entire system is then the union of solutions to each individual monomer Schrödinger equation.

The radial distribution function describes the probability of finding an atom at a particular distance from one reference atom and is of central importance for relating our vibrational calculation to thermodynamic quantities. Using the vibrational wavefunction, we can com-

pute the radial distribution function directly according to,

$$g(r) = \int \sum_{i \neq 0} (\delta(|\vec{r}_i - \vec{r}_0| - r))|\Psi|^2 d\tau, \tag{3}$$

where $\vec{r}_0$ is the position vector of the reference atom, $\vec{r}_i$ gives the coordinates of one of the remaining atoms of the system, and the wavefunction is integrated over all space. The sum of δ-functions insures that we count any atom that is a distance r from the reference atom. Since our wavefunction is numerically represented on a grid in normal coordinates, we evaluate the density $|\Psi(\vec{q})|^2$ at each grid point and convert the normal coordinates into Cartesian coordinates. The Cartesian coordinates allow us to calculate the distances between the reference atom and all other atoms, which are the different values of r to which the contribution defined by the density is added to $g(r)$. Because it is not generally feasible to calculate a vibrational wavefunction for a fully coupled system, we apply this equation within our local-monomer model. The normal modes are thus the "local" modes for the monomer and the primary wavefunction we calculate is for the intramolecular motion. In order to include the effects of the intermolecular modes, which are not included in the LMM, we approximate the wavefunctions for these modes by the ground-state uncoupled harmonic oscillator wavefunctions. For a monomer with N atoms, this leads to a total wavefunction of the form

$$\Psi(q_1, q_2, \ldots, q_{3N}) = \phi(q_1) \cdots \phi(q_6) \psi(q_7, \ldots, q_{3N}), \tag{4}$$

where the $\phi(q_i)$ are the ground-state harmonic oscillator functions, $\psi(q_7, \ldots, q_{3N})$ is the coupled vibrational wavefunction for the intramolecular modes, and the q_i represent the local normal modes. We also note that the local monomer model as not restricted to the vibrational ground state and so we could potentially calculate RDFs with vibrationally excited states.

III. RESULTS AND DISCUSSION

We have applied the above approach to the four smallest hydrated chloride clusters, $(H_2O)Cl^-$, $(H_2O)_2Cl^-$, $(H_2O)_3Cl^-$, and $(H_2O)_4Cl^-$.

The $(H_2O)Cl^-$ PES and fully-coupled VCI calculations were reported in a previous publication. [33] We revisit it here to test the accuracy and effectiveness of the local-monomer approximation. In Table I we compare previous VCI calculations[33] on the full PES with

the vibrational energies obtained using the local-monomer approximation. To appreciate the magnitude of the shifts in the monomer energies due to presence of the chloride ion, we give the corresponding VCI energies of the free water monomer, using the semi-empirical Partridge-Schwenke potential [42] for reference. As seen, the error from the local monomer model is of the order of 10 cm^{-1}, which is much less than than the shift in these energies relative to the isolated H_2O.

For $(H_2O)_2Cl^-$ we located the global minimum geometry using the pairwise representation of the potential and show the configuration in Figure 1. Since the water monomers are in an acceptor/donor configuration with respect to one hydrogen bond, we will denote the water monomer which is donating the hydrogen as "donor" and the other water monomer as "acceptor". We have independently optimized the geometry using second-order Møller-Plesset perturbation theory (MP2) with the augmented correlation-consistent polarized triple ζ basis set [43, 44] (aug-cc-pVTZ) using the MOLPRO [45] suite of programs, and note that our results agree well with the previously reported MP2/aug-cc-pVDZ results of Xantheas. [46] The geometries obtained with our surface and from this optimization are in good agreement, as are the harmonic vibrational frequencies, shown in Table II.

Intramolecular H_2O vibrational energies were also calculated for this cluster using the LMM and here there are no benchmarks with which to compare. The results, given in Table III, show interesting and significant differences for the two monomers. For most modes the acceptor H_2O energies are more red-shifted than the corresponding ones for the donor, with the exception of the asymmetric stretch.

In Figure 2 we show comparisons between the 0 K radial distribution functions (RDF) calculated for $(H_2O)_2Cl^-$ using the local-monomer model (LMM) and benchmark full-dimensional path integral Monte Carlo (PIMC). The PIMC simulations at 6.25 K were used as a benchmark for the quantum mechanical RDFs. This temperature is low enough to ensure that there is no population in vibrationally excited modes. Evaluation of the density operator requires that the effective inverse temperature β/P, where P is a parameter, be sufficiently small[47] and here we used a value of $P = 2^{12} = 4096$. The Monte Carlo procedure was carried out using the standard Metropolis sampling methods[48] and the staging algorithm to sample paths.[49] For the staging parameter we choose a value of 12 which yielded a 39% acceptance ratio.

The LMM RDFs show remarkable agreement with the PIMC results and serve to empha-

size the importance of including the intermolecular modes in this calculation. The distribution obtained directly from the LMM vibrational wavefunction, including only intramolecular modes, (not shown) is narrower than the distribution shown due to the artificial absence of the intermolecular modes between the chloride anion and the water monomers. These modes are associated with the frustrated translations and rotations, and they allow the monomer some freedom to move relative to the fixed system and thus contribute significantly to the broadening of the observed RDFs. Inclusion of the 6 intermolecular modes raises the complexity of the integration, and in order to evaluate the resulting 9-dimensional integral, we employ Monte-Carlo integration. The individual components of the RDF are shown in Figure 3. The donor and acceptor waters have slightly different geometries and so each gives a unique contribution to the total RDF. The broad peak at approximately 2.1 Å corresponds to the hydrogen bridging the oxygen and chlorine atoms, while the peak (or shoulder) occurring between 3.0 and 3.5 Å corresponds to either the free hydrogen or the hydrogen participating in the hydrogen bond between the two water monomers. The oxygen appears as the sharp peak near 3.0 Å.

For $(H_2O)_3Cl^-$ and for $(H_2O)_4Cl^-$ we employ two different versions of the water-chloride potential. In the first version, we use a 2-body description for both the water-chloride and the water-water interaction. In the second version, we include a 3-body term in the water-water interaction which accounts for the majority of non-pairwise additive effects on the water-water potential energy surface. In both cases, the inclusion of 3-body effects does not significantly alter the minimum geometry, but does introduce improvements to the harmonic frequencies.

For $(H_2O)_3Cl^-$ we obtain the global minimum shown in Figure 4. The minimum has C_3 symmetry with all three water monomers occupying equivalent positions. The three water monomers form the base of a trigonal pyramid with the chloride anion at its apex. This geometry agrees well with previously reported *ab initio* minimum searches. [46, 50, 51] The harmonic frequencies on our PES also agree quite well with those reported at the MP2/aVDZ level of theory and basis, as shown in Table IV. The LMM vibrational energy levels are shown in Table V. Also we note that for both $(H_2O)_2Cl^-$ and $(H_2O)_3Cl^-$ we are also able to find the additional local minima reported by Xantheas, however we have not subjected these stationary points to the same analysis as the global minimum for each cluster.

We also calculated the 0 K RDFs, and these are shown in Figure 5. Comparing these with those for the binary water cluster, we see only small differences between them. Clearly these RDFs reflect the zero-point probability densities, and we expect that they will continue to be the dominant contributors to the RDFs at non-zero temperatures. Even at 0 K, there is considerable broadening due to zero-point probability densities, which warrants a comparison with classical results that neglect this quantum effect. Comparison of the present RDFs with those calculated at 250 K, by Tobias *et al.*, using Car-Parinello direct dynamics[52] show remarkable similarity although the present RDFs are still broader. This would seem to indicate that the zero-point probability distribution is still at least of equal importance to the total RDF, since the classical broadening due to geometry changes is still on a smaller scale than the zero-point broadening. As the temperature is increased, the RDF will become broader as the intermolecular modes are excited and the water molecules are able to sample a wider array of configurations, as can be seen from bulk classical simulations [5, 27, 53]. For the intramolecular modes, the RDF is likely to be dominated by the zero-point probability even at higher temperatures since it is harder to thermally populate their excited vibrational levels.

Finally, for $(H_2O)_4Cl^-$ we obtain the global minimum shown in Figure 6. The minimum has C_4 symmetry, where the chloride sits at the apex of pyramid with the four water molecules arranged so that each has two hydrogen bonds with neighboring waters and one hydrogen bond to the chloride. The harmonic frequencies on the PES are shown in Table VI. For the LMM vibrational calculations, all four water molecules are equivalent, so results for only one are shown in Table VII. The results using the PES with 3-body water-water interactions are generally slightly better than those using only 2-body water-water interactions although the differences are small. Comparing the series involving two, three, and four waters, we see that the water-water interactions become progessively more important. The shift of the OH vibrational frequency due to the ionic nature of the hydrogen bond formed with chloride lessens and the shift due to the hydrogen bonding between waters increases.

IV. CONCLUSIONS

We reported the development of *ab initio* potential energy surfaces for microhydrated chloride, which we believe are an important step towards an *ab initio* description of electrolyte

solutions. The potentials include highly accurate and flexible 2 and 3-body water terms and are able to accurately reproduce geometries and frequencies for the clusters H_2OCl^-, $(H_2O)_2Cl^-$, $(H_2O)_3Cl^-$, and $(H_2O)_4Cl^-$. We have also demonstrated that the local-monomer model is capable of giving accurate predictions of vibrational frequencies, which will be of significant importance in calculating properties for bulk solutions. Finally, we have shown that we can calculate radial distribution functions using the vibrational wavefunctions obtained within the local-monomer approximation.

We believe this work can readily be extended to develop *ab initio* surfaces for the interaction of various cations and anions with water, with which we will study the properties of bulk solutions. This approach contains a number of particularly attractive features: it gives an accurate description of aqueous solutions that is readily compatible with quantum mechanical calculation of the vibrational wavefunction, it can be systematically improved by the incorporation of 3- or higher-body effects, and it obviates the need to *a priori* identify the forces and corresponding functional forms that will be important.

Acknowledgments

We thank the National Science Foundation (CHE-0848233) for financial support.

[1] Ando, K.; Hynes, J. T. *Adv. Chem. Phys.* **1999**, *110*, 381.

[2] Koneshan, S.; Rasaiah, J. C.; Lynden-Bell, R. M.; Lee, S. H. *J. Phys. Chem. B* **1998**, *102*, 4193.

[3] Heisler, I. A.; Meech, S. R. *Science* **2010**, *327*, 857.

[4] Jungwirth, P.; Tobias, D. J. *J. Phys. Chem. B* **2001**, *105*, 10468.

[5] Wick, C. D.; Xantheas, S. S. *J. Phys. Chem. B* **2009**, *113*, 4141.

[6] Bhatt, D.; Chee, R.; Newman, J.; Radke, C. J. *Curr. Opinion Colloid Interface Sci.* **2004**, *9*, 145.

[7] Tobias, D. J.; Hemminger, J. C. *Science* **2008**, *319*, 1197.

[8] Ghosal, S.; Hemminger, J. C.; Bluhm, H.; Mun, B. S.; Hebenstreit, E. L. D.; Ketteler, G.; Ogletree, D. F.; Requejo, F. G.; Salmeron, M. *Science* **2005**, *307*, 563.

[9] Park, S.; Fayer, M. D. *Proc. Natl. Acad. Sci.* **2007**, *104*, 16731.

[10] Smith, J. D.; Saykally, R. J.; Geissler, P. L. *J. Am. Chem. Soc.* **2007**, *129*, 13847.

[11] Jungwirth, P.; Tobias, D. J. *J. Phys. Chem. B* **2002**, *106*, 6361.

[12] Warshel, A.; Levitt, M. *J. Mol. Biol.* **1976**, *103*, 227.

[13] Caldwell, J.; Dang, L. X.; Kollman, P. A. *J. Am. Chem. Soc.* **1990**, *112*, 9144.

[14] Lamoureux, G.; MacKerell, A. D.; Roux, B. *J. Chem. Phys.* **2003**, *119*, 5185.

[15] Paricaud, P.; Predota, M.; Chialvo, A. A.; Cummings, P. T. *J. Chem. Phys.* **2005**, *122*, 244511.

[16] Iuchi, S.; Izvekov, S.; Voth, G. A. *J. Chem. Phys.* **2007**, *126*, 124505.

[17] Car, R.; Parrinello, M. *Phys. Rev. Lett.* **1985**, *5*, 2471.

[18] Kuo, I.-F. W.; Mundy, C. J. *Science* **2004**, *303*, 658.

[19] VandeVondele, J.; Mohamed, F.; Krack, M.; Hutter, J.; Sprik, M.; Parrinello, M. *J. Chem. Phys.* **2005**, *122*.

[20] Lee, H.-S.; Tuckerman, M. E. *J. Chem. Phys.* **2007**, *126*, 164501.

[21] Kropman, M. F.; Bakker, H. J. *J. Chem. Phys.* **2001**, *115*, 8942.

[22] Kropman, M. F.; Bakker, H. J. *Science* **2001**, *291*, 2118.

[23] Park, S.; Moilanen, D. E.; Fayer, M. D. *J. Phys. Chem. B* **2008**, *112*, 5279.

[24] Auer, B.; Schmidt, J. R.; Skinner, J. L. *Proc. Nat. Acad. Sci. USA* **2007**, *104*, 14215.

[25] Auer, B.; Skinner, J. L. *J. Chem. Phys.* **2008**, *128*, 224511.

[26] l. C. Jansen, T.; Auer, B. M.; Yang, M.; Skinner, J. L. *J. Chem. Phys.* **2010**, *132*, 224503.

[27] Lin, Y.-S.; Auer, B. M.; Skinner, J. L. *J. Chem. Phys.* **2009**, *131*, 144511.

[28] Braams, B. J.; Bowman, J. M. *Int. Rev. Phys. Chem.* **2009**, *28*, 577.

[29] Huang, X.; Braams, B. J.; Bowman, J. M. *J. Phys. Chem. A* **2006**, *110*, 445.

[30] Huang, X.; Braams, B. J.; Bowman, J. M.; Kelly, R. E. A.; Tennyson, J.; Groenenboom, G. C.; van der Avoird, A. *J. Chem. Phys.* **2008**, *128*, 034312.

[31] Shank, A.; Wang, Y.; Kaledin, A.; Braams, B. J.; Bowman, J. B. *J. Chem. Phys.* **2009**, *130*, 144314.

[32] Wang, Y.; Shepler, B. C.; Braams, B. J.; Bowman, J. M. *J. Chem. Phys.* **2009**, *131*, 054511.

[33] Rheinecker, J.; Bowman, J. M. *J. Chem. Phys.* **2006**, *125*, 133206.

[34] Wang, Y.; Bowman, J. M. *Chem. Phys. Lett.* **2010**, *491*, 1.

[35] Salmi, T.; Haenninen, V.; Garden, A. L.; Kjaegaard, H. G.; Tennyson, J.; Halonen, L. *J.*

Phys. Chem. A **2008**, *112*, 6305.

[36] Salmi, T.; Kjaergaard, H. G.; Halonen, L. *J. Phys. Chem. A* **2009**, *113*, 9142.

[37] Salmi, T.; Runeberg, N.; Halonen, L.; Lane, J. R.; Kjaergaard, H. G. *J. Phys. Chem. A* **2010**, *114*, 4835.

[38] Kumar, R.; Skinner, J. L. *J. Phys. Chem. B* **2008**, *112*, 8311.

[39] Bowman, J. M.; Carrington, T.; Meyer, H.-D. *Mol. Phys.* **2008**, *106*, 2145.

[40] Romanowski, H.; Bowman, J. M.; Harding, L. B. *J. Chem. Phys.* **1985**, *82*, 4155.

[41] Watson, J. K. G. *Mol. Phys.* **1968**, *15*, 479.

[42] Partridge, H.; Schwenke, D. W. *J. Chem. Phys.* **1997**, *106*, 4618.

[43] Dunning, T. H. *J. Chem. Phys.* **1989**, *90*, 1007.

[44] Kendall, R. A.; Dunning, T. H.; Harrison, R. J. *J. Chem. Phys.* **1992**, *96*, 6796.

[45] < MOLPRO 2002.6. Werner, H.-J.; Knowles, P.; Lindh, R.; Schütz, M.; others. **2003**.

[46] Xantheas, S. S. *J. Phys. Chem.* **1996**, *100*, 9703.

[47] Ceperley, D. M. *Rev. Mod. Phys.* **1995**, *67*, 279.

[48] Metropolis, N.; Rosenbluth, A. W.; Rosenbluth, M. N.; Teller, A. H.; Teller, E. *J. Chem. Phys.* **1953**, *21*, 1087.

[49] Janke, W.; Sauer, T. *J. Chem. Phys.* **1997**, *107*, 5821.

[50] Gora, R. W.; Roszak, S.; Leszczynski, J. *Chem. Phys. Lett.* **2000**, *325*, 7.

[51] Kemp, D. D.; Gordon, M. S. *J. Phys. Chem. A* **2005**, *109*, 7688.

[52] Tobias, D. J.; Jungwirth, P.; Parrinello, M. *J. Chem. Phys.* **2001**, *114*, 7036.

[53] Benjamin, I. *J. Chem. Phys.* **1991**, *95*, 3698.

[54] Roscioli, J. R.; Diken, E. G.; Johnson, M. A.; Horvath, S.; McCoy, A. B. *J. Phys. Chem. A* **2006**, *110*, 4943.

TABLE I: Comparison of vibrational frequencies (in cm^{-1}) for $(H_2O)Cl^-$ between exact vibrational CI on our PES [33], denoted PES-VCI, the local-monomer model, denoted LMM-VCI, and experiment [54]. For reference we also provide the vibrational frequencies of the free water monomer from the potential of Partridge and Schwenke. [42]

Mode	PES-VCI	LMM-VCI	Expt.	Free H_2O
HOH Bend	1660	1656	1650	1595
HOH Bend overtone	3308	3281	3283	3151
symmetric OH stretch	3123	3093	3130	3657
asymmetric OH stretch	3681	3681	3690	3756

TABLE II: Comparison between harmonic frequencies on our PES and those calculated using MP2/aVTZ for $(H_2O)_2Cl^-$. All frequencies are in cm^{-1}.

PES	MP2/aVTZ
109	100
125	155
177	179
218	215
355	357
409	410
451	469
688	674
763	811
1718	1660
1733	1694
3387	3311
3461	3589
3805	3794
3840	3883

TABLE III: Local-monomer model VCI vibrational energies of each water monomer in $(H_2O)_2Cl^-$. All frequencies are in cm^{-1}.

Mode	Donor H_2O	Accepter H_2O
ν_{bend}	1668	1652
ν_{sym}	3173	3097
$2\nu_{\text{bend}}$	3302	3268
ν_{asym}	3621	3662
$\nu_{\text{bend}} + \nu_{\text{sym}}$	4791	4692
$3\nu_{\text{bend}}$	4904	4850
$\nu_{\text{bend}} + \nu_{\text{asym}}$	5277	5305
$2\nu_{\text{sym}}$	6054	5910
$2\nu_{\text{bend}} + \nu_{\text{sym}}$	6367	6241

TABLE IV: Comparison between harmonic frequencies on our PES and those calculated using MP2/aVDZ [46] for $(H_2O)_3Cl^-$. All frequencies are in cm^{-1}.[a]

MP2/aVDZ	PES (2-body)	PES (2 and 3-body)
[2] 96	[2] 101	[2] 115
128	130	136
[2] 163	[2] 176	[2] 179
207	230	232
[2] 372	[2] 349	[2] 384
425	427	[2] 421
[2] 446	[2] 403	436
661	609	643
[2] 708	[2] 717	[2] 731
804	775	804
[2] 1676	[2] 1724	[2] 1760
1692	1751	1732
[2] 3553	[2] 3471	3480
3581	3440	[2] 3489
3733	3781	3758
[2] 3749	[2] 3789	[2] 3771

[a] Numbers in brackets denote degeneracy.

TABLE V: Local-monomer model VCI vibrational energies of the water monomers in $(H_2O)_3Cl^-$. All three monomers are equivalent. All frequencies are in cm^{-1}.

Mode	LMM-VCI H_2O (2-body)	LMM-VCI H_2O (2 and 3-body)
ν_{bend}	1663	1664
ν_{sym}	3179	3219
$2\nu_{\text{bend}}$	3290	3301
ν_{asym}	3603	3584
$\nu_{\text{bend}} + \nu_{\text{sym}}$	4786	4832
$3\nu_{\text{bend}}$	4884	4913
$\nu_{\text{bend}} + \nu_{\text{asym}}$	5254	5239
$2\nu_{\text{sym}}$	6061	6193
$2\nu_{\text{bend}} + \nu_{\text{sym}}$	6346	6408

TABLE VI: Comparison between harmonic frequencies on our PES including 2-body or 3-body water terms and those calculated using MP2/aVDZ [46] for $(H_2O)_4Cl^-$. All frequencies are in cm^{-1}.[a]

MP2/aVDZ	PES (2-body)	PES (2 and 3-body)
59	45	51
103	107	115
[3] 114	[2] 118	[2] 132
186	132	139
[2] 188	149	174
202	[2] 192	[2] 198
[2] 390	227	229
397	325	369
399	[2] 394	[2] 403
438	405	416
[2] 562	418	423
644	[2] 469	[2] 516
681	610	658
[2] 727	686	706
845	[2] 709	[2] 730
1681	763	801
[2] 1695	[2] 1736	[2] 1741
1714	1744	1747
[2] 3603	1747	1755
3604	3457	3471
3614	[3] 3486	[2] 3502
3698	[3] 3774	3506
[2] 3699	3784	3745
3707		[2] 3749
		3760

[a] Numbers in brackets denote degeneracy.

TABLE VII: Local-monomder model for vibrational energies of the water monomers in $(H_2O)_4Cl^-$. All four monomers are equivalent. All frequencies are in cm^{-1}.

Mode	LMM-VCI H_2O (2-body)	LMM-VCI H_2O (2 and 3-body)
ν_{bend}	1667	1673
ν_{sym}	3194	3215
$2\nu_{\text{bend}}$	3296	3308
ν_{asym}	3591	3561
$\nu_{\text{bend}} + \nu_{\text{sym}}$	4801	4828
$3\nu_{\text{bend}}$	4891	4911
$\nu_{\text{bend}} + \nu_{\text{asym}}$	5247	5222
$2\nu_{\text{sym}}$	6078	6129
$2\nu_{\text{bend}} + \nu_{\text{sym}}$	6354	6388

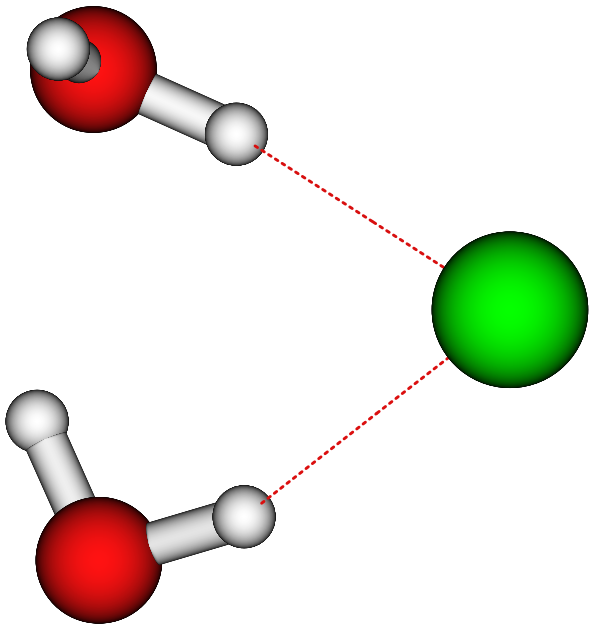

FIG. 1: Minimum geometry for $(H_2O)_2Cl^-$.

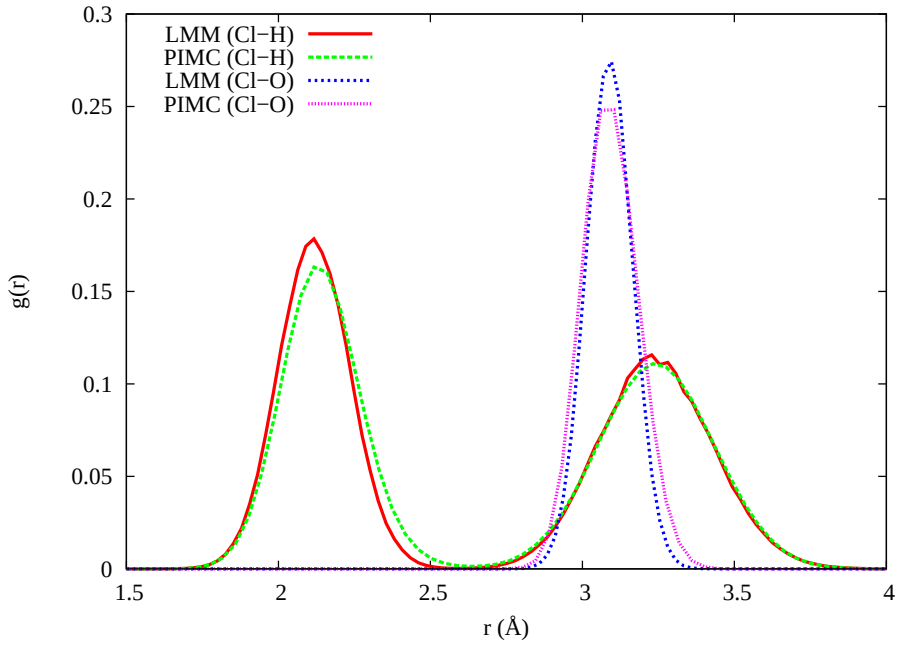

FIG. 2: Comparison of the radial distribution functions for $(H_2O)_2Cl^-$ calculated using the local monomer model (LMM) and full-dimensional path integral Monte Carlo (PIMC) at 6.5 K. The LMM RDF shows excellent agreement with the PIMC calculation.

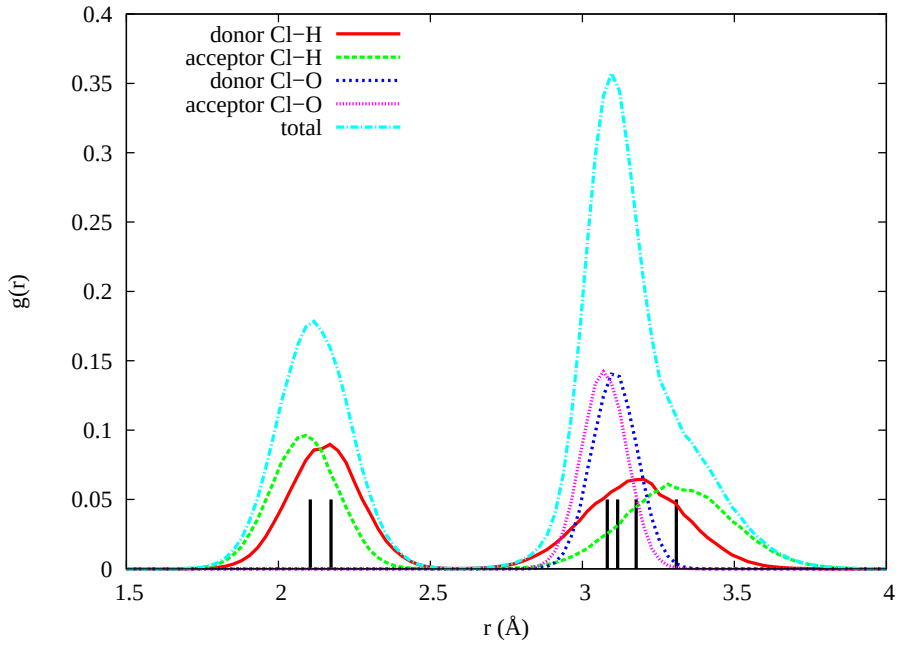

FIG. 3: Radial distribution function for $(H_2O)_2Cl^-$ between chlorine and the water hydrogen and oxygen atoms. The RDF includes the effect of a harmonic solution to the intermolecular modes and is calculated for the global minimum geomtry at 0 Kelvin. The sticks indicate the classical (0 K) position of the atoms.

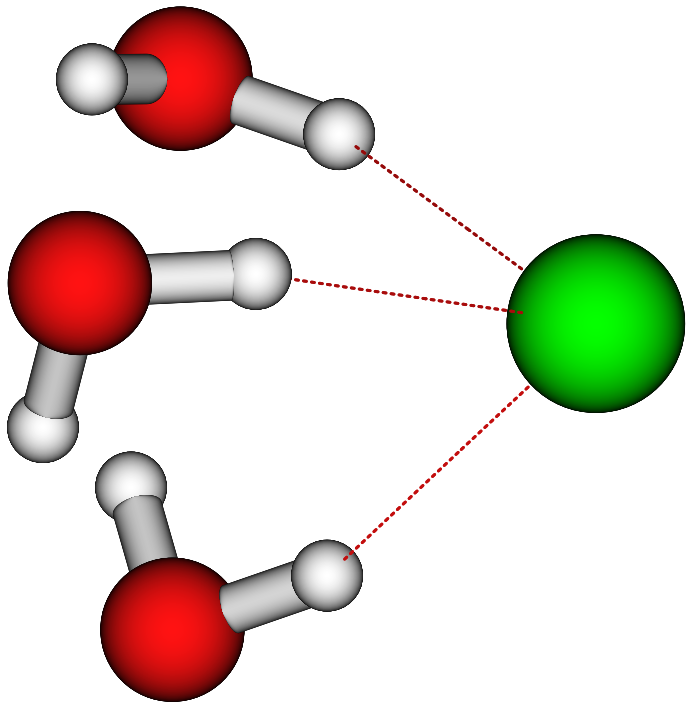

FIG. 4: Minimum geometry for $(H_2O)_3Cl^-$. The cluster has C_3 symmetry and the three water monomers form the base of a trigonal pyramid with the chloride anion at its apex.

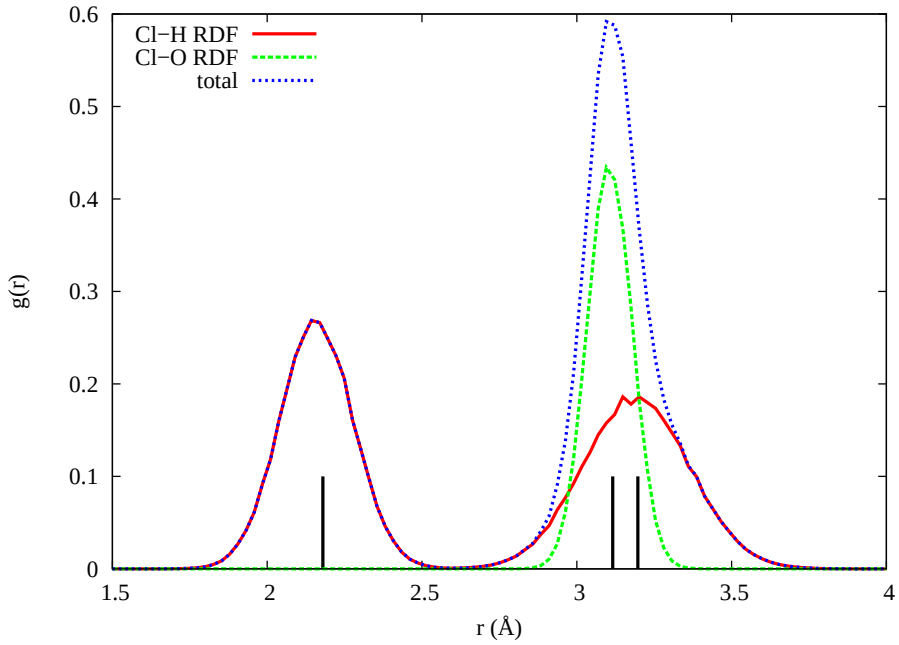

FIG. 5: Radial distribution function for $(H_2O)_3Cl^-$ between chlorine and the water hydrogen and oxygen atoms. All three water monomers are identical and so the total RDF is simply three times the RDF of one of the water molecules. The RDF shown includes a harmonic solution for the intermolecular modes and the sticks indicate the classical (0 K) position of the atoms.

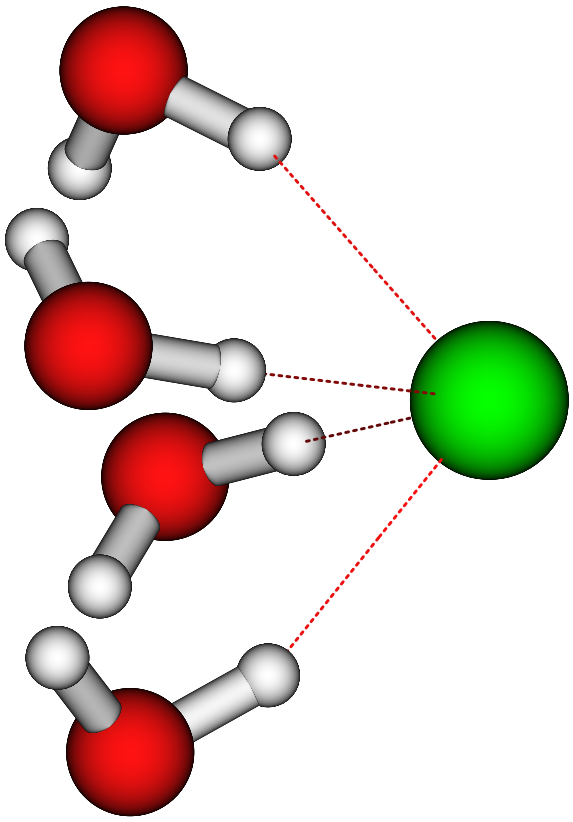

FIG. 6: Minimum geometry for $(H_2O)_4Cl^-$. The cluster has C_4 symmetry and the four water monomers form the base of a pyramid with the chloride anion at its apex.